ISSN 2070-2051, Protection of Metals and Physical Chemistry of Surfaces, 2017, Vol. 53, No. 6, pp. 1005–1014. © Pleiades Publishing, Ltd., 2017.
Original Russian Text © V.S. Rudnev, V.P. Morozova, I.V. Lukiyanchuk, I.A. Tkachenko, M.V. Adigamova, P.M. Nedozorov, 2017, published in Fizikokhimiya Poverkhnosti i Zashchita Materialov, 2017, Vol. 53, No. 6, pp. 606–615.

NANOSCALE AND NANOSTRUCTURED MATERIALS AND COATINGS

The Effect of Iron Precursors in an Electrolyte on the Formation, Composition, and Magnetic Properties of Oxide Coatings on Titanium

V. S. Rudnev[a, b, *], V. P. Morozova[a], I. V. Lukiyanchuk[a], I. A. Tkachenko[a], M. V. Adigamova[a], and P. M. Nedozorov[a]

[a] *Institute of Chemistry, Far Eastern Branch, Russian Academy of Sciences, Vladivostok, 690022 Russia*

[b] *Far Eastern Federal University, Vladivostok, 690950 Russia*

**e-mail: rudnevvs@ich.dvo.ru*

Received July 19, 2016

Abstract—The effect of iron sulfate and citrate addition into the base alkaline phosphate-borate-tungstate electrolyte on the peculiarities of plasma-electrolytic formation of coatings on titanium, their thickness, surface morphology, composition, and magnetic characteristics has been investigated. In the first electrolyte, dispersed particles of iron hydroxides and hydroxo salts are formed, whereas the second one comprises a true solution. Numerous Fe-containing crystallites of a size of ~50 nm united into agglomerates have been found in the suspension electrolyte with $FeSO_4$. Such coatings manifest ferromagnetic properties: coercive force H_c of the samples is 62 and 148 Oe at 300 and 2 K, respectively. In pores of the coatings obtained in the electrolyte with $FeC_6H_5O_7$ (true solution), the presence of crystallites is less clearly expressed, while crystallites themselves are larger and molten to a higher degree. At room temperature, such coatings are paramagnetic; at 2 K, they manifest ferromagnetic behavior with the H_c value of up to 200 Oe. The available data enable one to associate ferromagnetic properties of the formed coatings with metals concentrated in pores.

Keywords: titanium, plasma electrolytic oxidation, iron precursors, nano- and microcrystals, ferromagnetism

DOI: 10.1134/S2070205117060193

1. INTRODUCTION

Recently, researchers have demonstrated a significant interest in the establishment of formation regularities, composition, structure, and functional properties of Fe-containing oxide coatings formed on titanium, aluminum, and their alloys by the method of plasma-electrolytic oxidation (PEO) [1–15]. The PEO method consists in oxidation of the surface of metals and alloys in electrolytes under conditions of the effect of spark or microarc discharges in the near-electrode area [16–18]. Depending on the composition and structure, the obtained Fe-containing PEO coatings can have ferromagnetic [6, 7, 12], catalytic [13, 14], temperature-controlled [2, 10, 15], or decorative [15, 19] properties, improved wear resistance [11], or the capacity to absorb SHF radiation at specific wavelengths [1]. To obtain iron-containing oxide coatings by the single-stage PEO method, suspension electrolytes with particles of iron [1] or iron oxide (Fe_2O_3) [2, 3], true solutions with EDTA iron complexes [4–6], and colloid electrolytes with polyphosphate iron complexes [7] are used. Also, potassium hexacyanoferrate [8, 9, 19] and iron oxalate [7, 12], sulfate [10], or citrate [11] can be introduced into the electrolyte as the iron source.

As was shown in [7, 12], PEO coatings formed on aluminum and titanium in alkaline suspension electrolytes with iron oxalates manifested ferromagnetic properties. In these cases, the base alkaline aqueous electrolyte of the composition $Na_3PO_4 + Na_2B_4O_7 + Na_2WO_4$ (PBW electrolyte) was added with an aqueous solution of $Fe_2(C_2O_4)_3$. The hydrolysis processes yielded formation of negatively charged dispersed particles of Fe(III) hydroxide and hydroxo salts. In the formed coatings, iron imparting coatings with ferromagnetic properties is concentrated in coatings' defect surface sites and pores [7, 12]. In some cases, the presence of crystallites with the increased content of metals from the electrolyte and from the substrate was revealed [12, 20, 21]. The increased concentrations of iron and substrate along with low concentrations of oxygen in pore bottoms and walls, as well as in crystallites, allows it to be supposed that some of the metal atoms in pores are in a reduced state. The presence of reduced iron in coatings is corroborated by the results of X-ray photoelectron spectroscopy [20] and X-ray

diffraction analysis [12]. Fe-containing crystallites were not found in pores of coatings formed in the electrolyte upon removal of particles of iron hydroxides and hydroxo salts, while coatings contained low iron concentrations both over the surface and in pores and are paramagnetics at room temperature [22]. Thus, upon formation of PEO coatings in the alkaline PBW electrolyte with addition of $Fe_2(C_2O_4)_3$, the increased concentrations of iron in pores and defect surface sites are related to the presence of dispersed particles of iron hydroxides and hydroxo salts in solution [22]. Note that iron is also concentrated in pores and coatings manifest ferromagnetic properties in alkaline electrolytes of other compositions containing $Fe_2(C_2O_4)_3$ and forming dispersed hydroxide particles [23]. On the other hand, the quantity of iron embedded into pores, the element composition of dispersed particles and pore bottom and walls and the magnetic characteristics of coatings depend on the composition of the base electrolytes under study [23].

According to the data of [6], coatings with ferromagnetic characteristics can be also formed in true solutions containing complex EDTA–Fe^{3+} ions as the iron precursor. In this case, iron concentration in the pores of coatings was also registered [4].

Thus, iron-containing ferromagnetic coatings on aluminum and titanium can be formed both in electrolytes with dispersed particles of iron hydroxides and in true solutions containing EDTA–Fe^{3+} complexes. In both cases, iron concentrating in coating pores was registered. At the same time, the effect of different iron precursors in the alkaline electrolyte on the composition and magnetic properties of the formed PEO coatings has been studied insufficiently. In view of the above, the objective of the present work consisted in studies of the composition, structure, and magnetic properties of coatings formed in the PBW electrolyte with additions of $FeSO_4$ or $FeC_6H_5O_7$. In the first electrolyte, dispersed particles of iron hydroxides and hydroxo salts are formed, while the second one comprises a true solution.

2. MATERIALS AND METHODS

2.1. Electrolyte Preparation

To obtain coatings, two electrolytes were used. They contained (mol/L) $0.066Na_3PO_4$ + $0.034Na_2B_4O_7$ + $0.006Na_2WO_4$ + $0.03FeSO_4$ or $FeC_6H_5O_7$. Depending on the type of anion of the Fe-containing component, the working electrolytes are indicated as PBWFe-SO_4 and PBWFe-Citr, respectively. Electrolytes were prepared by solution mixing. In each case, 0.5 L of phosphate–borate–tungstate solution (PBW electrolyte [24]) with doubled component concentrations was added with 0.5 L of a solution of iron salt containing 0.06 mol/L $FeSO_4$ or $FeC_6H_5O_7$. To prepare the base electrolyte, commercial reagents were used: $Na_3PO_4 \cdot 12H_2O$, $Na_2B_4O_7 \cdot 10H_2O$ (chemically pure grade) and $Na_2WO_4 \cdot 2H_2O$ (analytic grade). Iron was added in the form of iron(II) sulfate ($FeSO_4 \cdot 7H_2O$) or iron(III) citrate ($FeC_6H_5O_7 \cdot 3H_2O$): all the reagents are of analytical grade. The prepared solutions were stirred for 1 h. The selection of added iron-salt concetrations (0.03 mol/L) was caused by the low solubility of iron (III) citrate.

Measurements of the values of pH and electrolyte electroconductivity were carried out using an S470-K SevenExcellence pH meter–conductometer (Mettler Toledo, Switzerland).

2.2. Coating Formation

Flat samples of titanium alloy VT1-0 of a size of $2 \times 2 \times 0.1$ cm were used. For surface standardization, prior to anodization, the samples were polished in a mixture of concentrated acids HF : HNO_3 = 1 : 3 (by volume) at 70°C five or six times with 0.50-min holding each time and intermediate washing with water until formation of a reflecting surface [25]. Upon chemical polishing, the sample were washed, first, with tap water and then with distilled water and were dried in air at 70°C.

The electrochemical cell for synthesis consisted of a vessel of a volume of 1 L made of a thermally resistant glass, a coil-shaped cathode made of a hollow nickel-alloy tube that also served as a cooler, and a magnetic stirrer. A computer-controlled TER4-100/460N device (Russia) operated in the unipolar mode served as a current source.

All the coatings were formed at anodic polarization of samples of VT1-0 titanium alloy in the galvanostatic mode with the effective current density of 0.05 A/cm^2 for 5 and 10 min. The electrolyte temperature during the plasma electrolytic process did not exceed 30°C.

2.3. Determination of Thickness, Coatings' Phase and Element Composition, and Pore Structure

The coating thickness was determined using a VT201 vortex-current thickness meter (Russia). X-ray diffraction analysis of samples with coatings was carried out using a D8 ADVANCE X-ray diffractometer (Germany) in CuK_α radiation. X-ray diffraction patterns were recorded at room temperature in angle range 2θ from 10° to 80° in two modes: (1) at a rate of 2°/min (standard recording) and (2) at increment scanning every 0.02° and time of signal accumulation in the point 10 s (recording with signal accumulation). To deconvolute the obtained spectra, the EVA-2 search program with the PDF-2 database was used.

The element-composition data and surface images were obtained using a JXA 8100 X-ray spectral analyzer (Japan) equipped with an INCA energy-dispersive accessory (United Kingdom). Prior to measurements, gold was sputtered on the surface to prevent

surface contamination. The averaged element composition was determined based on the results of scanning five randomly selected surface areas (~250 μm^2) at a depth of up to 5 μm each. The coating surface and the pore structure were also studied using a Hitachi S5500 high-resolution scanning electron microscope (Japan). The element composition of specific coating parts, including rolls around pores, formations inside them, and pore bottoms, was determined using a Thermo Scientific microscope accessory for energy-dispersive analysis (United States). The data were averaged for at least five selected similar relief objects.

2.4. Determination of Magnetic Characteristics

Magnetization of the samples with coatings was measured using a SQUID MPMS 7 magnetometer (Germany). During measurements, the sample plane was placed in parallel to the magnetic-field direction. The dependences of magnetic moment M (emu/g) on magnetic-field intensity H (Oe) were registered at temperatures of 300 and 2 K in fields of up to 50 kOe. For the magnetization calculation, the measured magnetic moment was normalized on the mass of the sample with coating. The mass fraction of coatings in samples was ~1–3%.

3. RESULTS AND DISCUSSION

3.1. Electrolyte States

The suspension electrolyte PBWFe-SO_4 is of hemp-green color. Aqueous solutions of Fe(II) sulfate are known to be of green color. The hemp-green color of the PBWFe-SO_4 electrolyte indicates the presence of hydroxides and hydroxo salts of both Fe(II) and Fe(III) in the solution. It is most probable that mixing the alkaline PBW electrolyte and the iron(II) solution yields, first, formation of dispersed particles of iron(II) hydroxides and hydroxo salts, some of which is oxidized to Fe(III) compounds at interaction with air oxygen [26]: $2Fe(OH)_2 + 1/2O_2 + H_2O \rightarrow 2Fe(OH)_3$.

An electrolyte with iron(III) citrate comprises a transparent solution of the orange-brown color. Note that, along with the electrolyte interaction, it started to opalesce and produced an insignificant quantity of precipitate, which can be related to titanium release into solution at PEO treatment, formation of colloid particles of hydrated titanium oxide, and sorption of electrolyte ions on them. Titanium dioxide is known to work as an adsorbent [27, 28]: in dependence on pH, positively or negatively charged active centers are present on its surface [29].

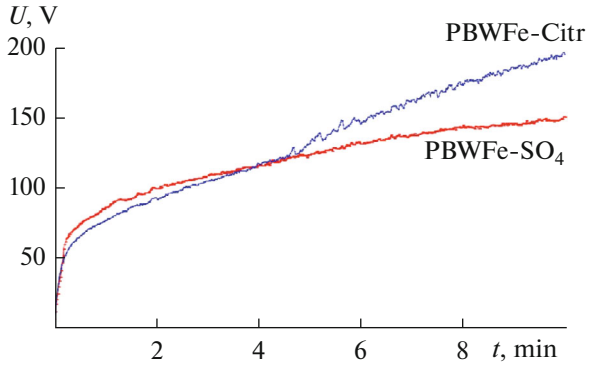

Fig. 1. Dependence of the voltage of coatings' formation on titanium on time in PBWFe electrolytes containing iron(II) sulfate or iron(III) citrate.

3.2. Voltage Chronograms

The graphs of dependences of the voltage on electrodes on time ($U = f(t)$) at coatings' formation in PBWFe electrolytes are shown in Fig. 1. Values of sparking voltages U_i were estimated from these graphs (Table 1). The dependence of $U = f(t)$ at formation of coatings in the PBWFe-SO_4 electrolyte have the shape characteristic of electrolytes weakly dissolving oxide of the treated metal [30, 31]. Dependence $U = f(t)$ for the PBWFe-Citr electrolyte is a curve with a bend. Such a curve behavior is characteristic of formation of PEO coatings in electrolytes that dissolve the growing oxide to a significant degree, as well as in the change of spark discharges to linear-spreading ones [32]. However,

Table 1. Electrolyte composition and characteristics of coatings formed at $i = 0.05$ A/cm^2 for $t = 5$ min (numerator) and $t = 10$ min (denominator)

Electrolyte	pH	ϰ, S/m	U_i, V	h, μm	C*, at %							H_c, Oe	
					C	O	Na	P	Ti	Fe	W	2 K	300 K
PBWFe-SO_4	10.2	1.63	70 ± 4	6.5 20.5	24.6 17.8	54.7 58.8	0.6 0.9	6.5 7.7	6.8 6.6	5.9 7.1	0.9 1.1	145 148	11 62
PBWFe-Citr	10.0	1.41	47 ± 3	16.1 28.0	16.6 13.1	60.2 61.8	0.7 1.0	8.5 9.4	6.8 6.5	6.2 7.0	1.0 1.2	201 141	16 21

ϰ is the electrolyte specific electroconductivity, U_i is the sparking voltage, h is coating thickness, and H_c is the coercive force.

* The coatings' element composition from the data of X-ray microprobe spectral analysis.

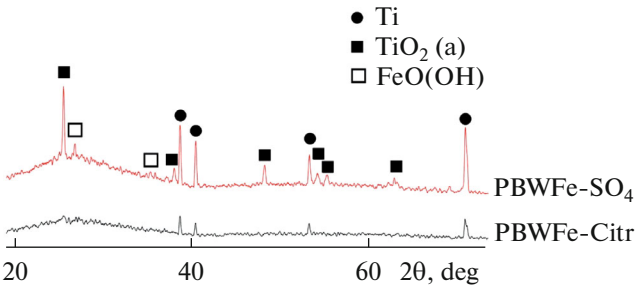

Fig. 2. X-ray diffraction patterns of titanium samples with PEO coatings formed within 10 min in PBWFe-SO_4 and PBWFe-Citr electrolytes.

formation of the secondary layer during the coatings' buildup was not visually observed.

3.3. Coating Thicknesses

The thicknesses of the formed coatings are shown in Table 1. Under identical conditions, the thickness of coatings formed in the PBWFe-Citr electrolyte is significantly larger than that of coatings in the suspension PBWFe-SO_4 electrolyte. In other words, citrate ions increase the rate of coatings' growth relative to the electrolyte with sulfate ions. The latter can be related to higher aggressiveness of the electrolyte with iron citrate with respect to titanium and its oxides that results in more expressed titanium dissolution, which makes possible the formation of looser thickened coatings or the emergence of spreading electric discharges and the growth of layered coatings [32]. According to [33], the emergence of spreading discharges is related to the fact that, in electrolytes with a high rate of etching of growing oxide, there a large number of structural defects emerge in the anodic layer, with their heterogeneous distribution inducing joint spark displacement. The hypothesis that the PBWFe-Citr electrolyte is highly aggressive toward the growing coating is in agreement with the behavior of the $U = f(t)$ curve (Fig. 1).

3.4. Coatings' Composition

The X-ray diffraction patterns of the coatings formed within 10 min are shown in Fig. 2. The XRD patterns obtained under standard registration conditions contain only reflections attributed to the substrate metal and a diffused halo in the angle range 2θ from 20° to 35°. Reflections attributed to anatase emerge, in addition, at registration with signal accumulation. In the case of the electrolyte with iron sulfate, the coatings' XRD patterns contain weak reflections that can be attributed to FeO(OH) in the akageneite.

From the data of X-ray microprobe spectral analysis (Table 1, the analysis depth up to 5 μm), the coatings formed in PBWFe-SO_4 and PBWFe-Citr electrolytes contain about the same concentrations of the analyzed elements. It is worth mentioning the higher phosphorus content and lower carbon one for the coatings formed in the citrate electrolyte. Taking into account the electrolyte composition, the coatings' element composition, and the obtained XRD patterns, one can suggest that the diffused halo is related to the presence of amorphous phosphates, borates, or oxide (including titanium and iron oxides) in the coatings.

In both cases, coatings contain significant carbon concentrations. In general, the presence of carbon in coatings or on their surface may be caused by three factors: surface contamination during manipulations with samples, sorption of carbon-containing compounds from the atmosphere on the surface, and carbon embedding into coatings during PEO. Embedding of carbon from electrolytes with iron citrate may be related to thermolysis of $C_3H_5O(COO)_3^{3-}$ anions in areas adjacent to electric-breakdown channels. The presence of carbon in coatings formed in electrolytes with iron sulfate can be explained by thermolysis of anions of carbonic acid present in the electrolyte due to CO_2 absorption from air. Since, from the data of [34, 35], we see that carbon is present both on the surface and in the bulk of PEO coatings, all three factors of its embedding can occur. It is worth noting that the measured carbon contents do not contradict the data of [34, 35] obtained for coatings formed in electrolytes of different compositions.

3.4. Surface Morphology and Characteristic Formations' Composition

Microphotographs of the coatings are shown in Fig. 3. Pore mouths of sizes of up to 10 μm (traces of breakdown channels) surrounded by rolls of the molten material are present on the coatings' surfaces. Dispersed particles (shown with arrows on the microphotographs) are discernible inside some of the pores. The increase of the time of formation results in enlargement of surface fragments: rolls around pores and height differences between elevations and cavities. Along with the increase of the formation time, one can note the decrease of total number of pores (predominantly of small sizes) on the surface.

Studies performed using a high-resolution microscope equipped with an attachment for energy-dispersive analysis allowed revealing the peculiarities of the composition and structure of morphological objects on the coating surface (see Figs. 4, 5).

Dispersed formations are present in most of the studied coatings' pores (see Fig. 4). In pores of coatings formed within 10 min, such formations comprise conglomerates consisting of large numbers of particles (crystallites) of sizes of 20–50 nm (Figs. 4b–4d). Along with an increase of the formation time up to 10 min, the number of crystallites in pores increases,

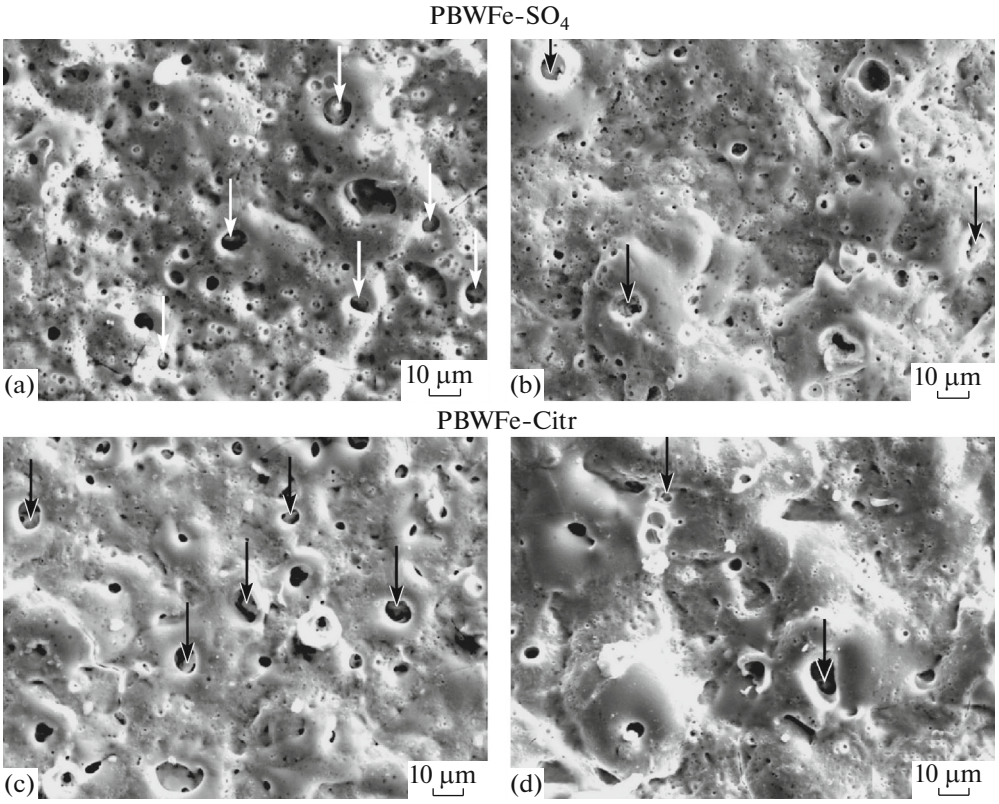

Fig. 3. Microphotographs of coatings formed in (a, b) PBWFe-SO_4 and (c, d) PBWFe-Citr electrolytes in (a, c) 5 and (b, d) 10 min. Arrows indicate dispersed particles in pores.

and they virtually completely fill the analyzed pore space, Similar formations can be seen on the coating surface around pores as well (Fig. 4b, shown with an arrow).

In pores of coatings formed in the PBWFe-Citr electrolyte, one also observes dispersed formations, but they appear to be less crystallized (molten to a greater degree) (Fig. 5). One should note that, here, the number of pores with discernible dispersed formations is smaller than in the case of coatings formed in the PBWFe-SO_4 electrolyte.

Figure 6 shows the diagrams reflecting the compositions of pores and surface of the coatings. The data on the surface composition were obtained from areas

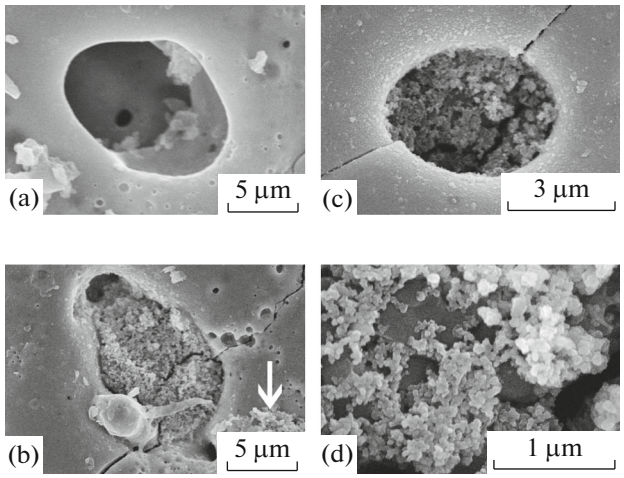

Fig. 4. SEM images of the surface of coatings formed in the PBWFe-SO_4 electrolyte in (a) 5 and (b–d) 10 min.

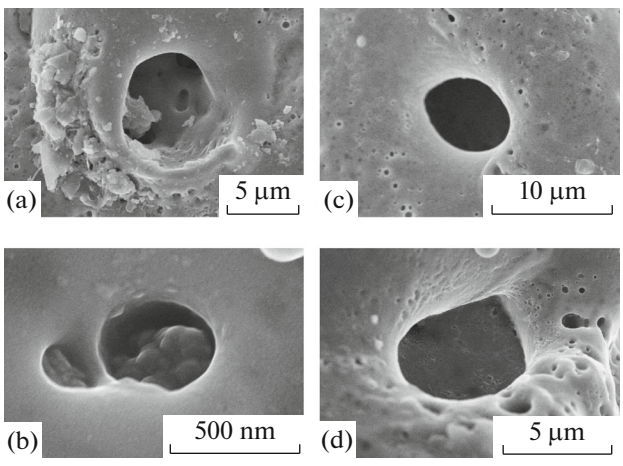

Fig. 5. SEM images of the surface of coatings formed in the PBWFe-Citr electrolyte in (a, b) 5 and (c, d) 10 min.

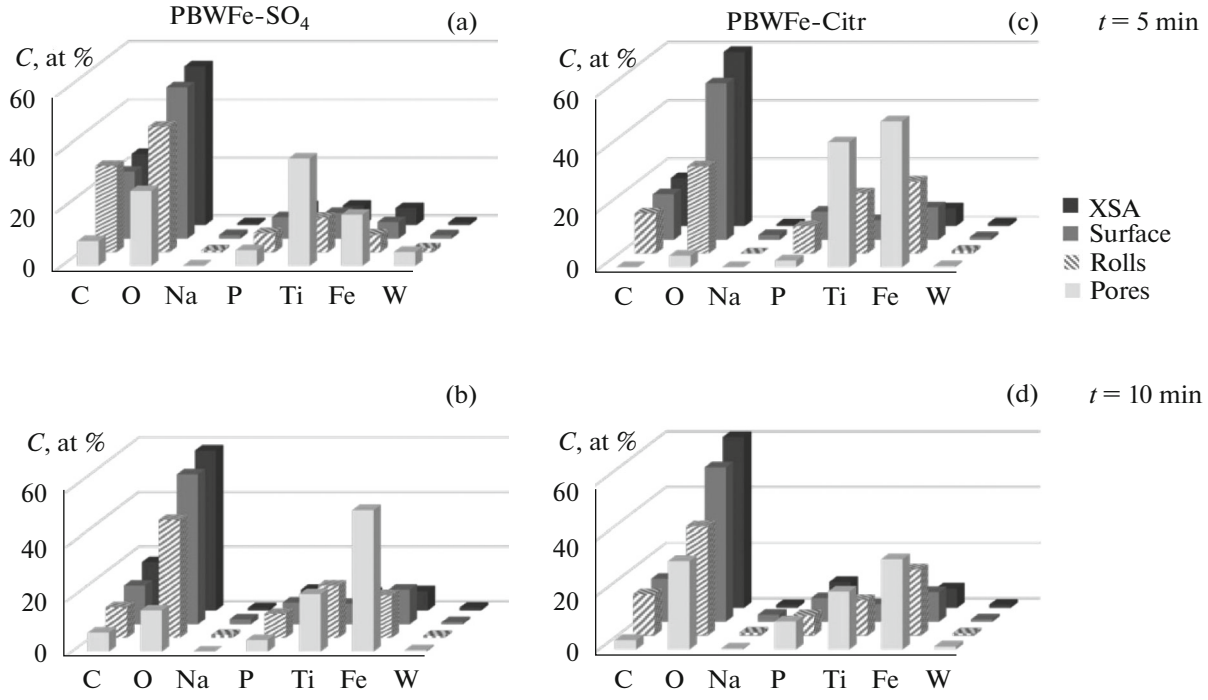

Fig. 6. Diagrams of element distribution on morphological objects of the surface of coatings formed in (a, c) 5 and (b, d) 10 min in (a, b) PBWFe-SO_4 and (c, d) PBWFe-Citr electrolytes from the data of energy-dispersive analysis (averaged compositions for pores, rolls, and surface are presented). For comparison, the composition of the surface from the data of X-ray microprobe spectral analysis (XSA) is also shown (Table 1).

of a size of 60 × 80 μm. For comparison, the diagrams show the surface composition from the data of X-ray microprobe spectral analysis (Table 1). The pore composition was obtained through averaging the data for the pores with dispersed particles (examples are presented in Figs. 4a–4c, 5a, 5b) and those without visible dispersed particles (examples in Figs. 5c, 5d). In the latter case, the compositions of pore bottom and walls were taken into account.

Analysis of the diagrams shows that, in all cases, the concentrations of iron and titanium in pores are significantly higher, while the oxygen concentration is lower, than on the surface. For example, crystallites in pores of coatings obtained within 10 min in the PBWFe-SO_4 electrolyte contain, at %, 51.9 Fe, 21.2 Ti, and just 15.1 O (Fig. 6b). From the data of energy-dispersive analysis, the contents of elements on the surface of such coatings are, at %, 12.7 Fe, 7.6 Ti, and 55.0 O. Since the quantity of oxygen in crystallites is insufficient for iron and titanium oxide formation, one can conclude that crystallites contain predominantly reduced metals. The data on the surface composition obtained using an energy-dispersive accessory to the scanning electron microscope and the method of microprobe analysis are virtually identical. The concentrations of titanium, iron, and oxygen in the rolls' composition are intermediate between those for pores and surface.

Similar data of the significantly higher contents of iron and titanium in pores as compared to the surface were earlier obtained for coatings formed on aluminum and titanium in PBW + $Fe_2(C_2O_4)_3$ electrolyte [12, 20].

The composition of formations on the surface of coatings similar to crystallites in pores (Fig. 4b) is as follows, at %: 31.8 C, 35.4 O, 4.9 P, 4.3 Ti, 22.0 Fe, and 0.7 W. The iron concentration in the composition of the formation to be analyzed has an intermediate value between those on the surface and in the pore. The existence of such formation may be related to the material release from the pore during spark or microarc discharges. Earlier, similar formations were observed around pores (breakdown channels) on the surface of PEO coatings on aluminum and titanium [36].

3.6. Coatings' Magnetic Characteristics

The magnetization curves of samples with coatings and magnetization temperature dependences are shown in Fig. 7. At room temperature, the coatings formed in the PBWFe-Citr electrolyte are paramagnetics, which is indicated by the linear dependence of magnetization on the field intensity and small values of H_c (Table 1), while at low temperatures they manifest ferromagnetic properties (the presence of hysteresis on field dependences of magnetization and the H_c value from 140 to 200 Oe). At low temperatures, the

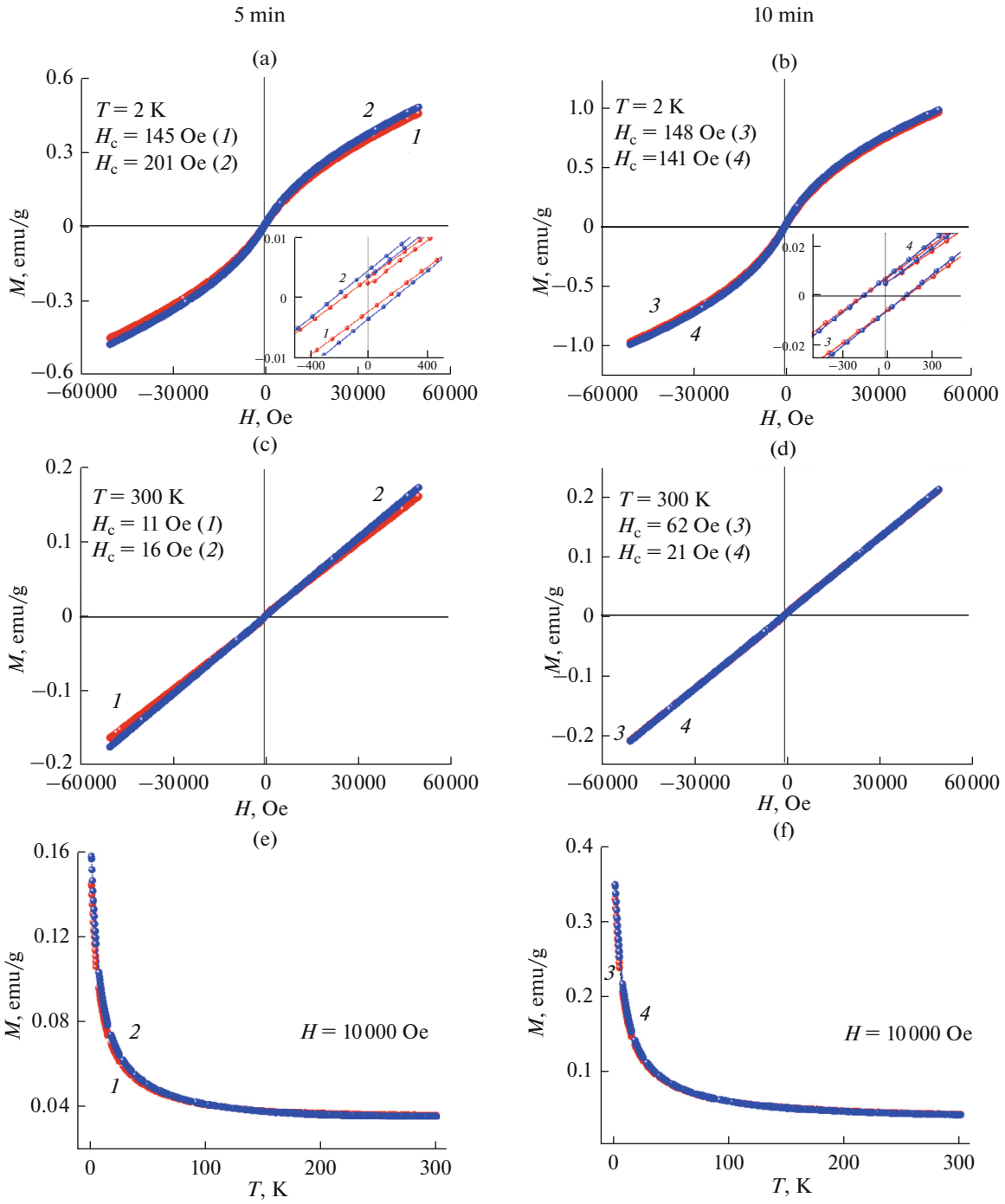

Fig. 7. Dependences of magnetic moment M of the samples with PEO coatings on (a-d) magnetic-field intensity H at (a, b) 2 and (c, d) 300 K and (e, f) temperature T at $H = 10000$ Oe. The coatings were formed in (a, c, e) 5 and (b, d, f) 10 min in the electrolytes: (*1*, *3*) PBWFe-SO_4 and (*2*, *4*) PBWFe-Citr. Inserts (a, b) show the small-field area.

coatings in the PBWFe-SO_4 electrolyte are ferromagnetics (H_c ~ 145 Oe). At room temperature, for the coatings obtained in this electrolyte, one observes the dependence of the coercive force on the formation time (Table 1). The latter can be related to sizes of iron-containing crystallites in the coating pores. The peculiarity of the behavior of magnetization curves at low temperatures consists in the absence of attainment of a saturation characteristic of ferromagnetics. The latter can be the result of the presence of superparamagnetic particles or those with antiferromagnetic properties in coatings, including pores. This assumption cor-

roborates the behavior of temperature dependences of samples magnetization in the stationary magnetic field. A dramatic increase of magnetization is observed at temperatures below ~50 K, which must be related to the contribution of superparamagnetic particles or antiferromagnetic–ferromagnetic transitions.

It is worth mentioning that for samples with ferromagnetic properties 'Fe-containing coating/Ti' formed in the PBW + 0.04 mol/L $Fe_2(C_2O_4)_3$ suspension electrolyte the coercive force values determined at room temperature and at those around the liquid helium level (2–10 K) were equal to 50–100 and 260–360 Oe, respectively [7, 20, 22]. In other words, the magnetic characteristics of the samples under study obtained in the present work do not contradict the earlier-obtained results for the coatings formed in alkaline suspension electrolytes with dispersed particles of iron and hydroxo salts. In addition, the coatings' magnetic characteristics are affected by the concentration of iron oxalate introduced into the PBW electrolyte [12]. In view of this, note that, in the present work, we used 0.03 mol/L Fe(II) or Fe(III), while in [7, 20, 22] the Fe(III) concentration was 0.08 mol/L.

To sum up, the data obtained in the present work and available in the literature [4–7, 12, 20, 22] enable one to conclude that, independently of the nature of the studied iron precursors and the state of the alkaline electrolyte (true solution or suspension electrolyte), iron, in all cases, concentrates predominantly in defect sites and pores of PEO coatings. Aside from iron, coatings' pores contain other metals from the electrolyte components or substrate. In many cases, pores of such coatings contain dispersed particles with increased metal contents. The oxygen deficiency in coatings' pores and the particles inside them allows assuming on the presence of metals in the reduced state. A majority of the studied coatings manifest ferromagnetic behavior at both low and room temperatures.

4. DISCUSSION

In general, the observed coatings' magnetic properties may be related to the presence of particles of reduced iron or its magnetoactive compounds contained in different morphological formations on the surface: pores (also, in dispersed particles inside pores), rolls, dispersed particles on the surface, and in the coating bulk. Since iron is apparently concentrated in pores (breakdown channels) (see Fig. 6), while pores occupy [37] about 20% of the surface, one has grounds to think that it is the iron in pores that determines the coatings' magnetic properties.

In the coating bulk, iron must be present in the composition of oxides and other insoluble oxygen-containing iron compounds, for example, akageneite (Fig. 2) or phosphates in the case of application of electrolytes with polyphosphates [7]. One should not exclude the presence of other iron compounds in the cases under study (for example, maghemite, magnetite, and titanomagnetite), but the used instrumental methods of analysis do not corroborate this presence.

Pores contain dispersed particles with increased concentrations of iron and titanium and a decreased one of oxygen. Such particles may consist of a mixture of reduced metals with their oxides or hydroxides. For example, taking into account the features of the PEO process, they comprise a metal core encapsulated into an oxide–hydroxide shell. Note that pores, both with dispersed particles and without them, can be present on the coating surface. In pores without visible dispersed particles, the composition of the pore bottom determined by the method of energy-dispersed analysis corresponds to the composition of dispersed particles. One can assume that, in the course of electrolyte components, entering the pores during spark or microarc discharges, they are thermally transformed under reducing-atmosphere conditions. The reducing properties can be provided by the excess of hydrogen in the moment of emission emerging due to water thermolysis [38] or by carbon present in the composition of many studied precursors. The thermal-transformation products must cover pore bottoms and walls and, in some cases, form dispersed particles available in pores. The latter is especially characteristic at formation of coatings in electrolytes releasing hydroxides and hydroxo salts of transition metals into precipitates.

The pores of coatings and dispersed particles have high contents of the substrate metal, for example, titanium (as in our case) or aluminum [12]. In general, this can occur both due to diffusion of the substrate metal from it or from lower oxide layers at increased temperatures accompanying discharge phenomena and because of the titanium transfer from the electrolyte bulk. During the PEO process, significant concentrations of the treated metal are known to be observed in the electrolyte [39, 40]. In the case of alkaline electrolytes, titanium transferred into the solution will be present in the form of hydroxide compounds. In the alkaline medium, negatively charged titanium hydroxides will also be transferred into breakdown areas and participate in formation of PEO coatings.

The observed features of the structure of some morphological formation on the surface and of coatings in general are of interest for development of ideas concerning the mechanism of growth of multicomponent PEO coatings in suspension electrolytes. During the discharge emergence, dispersed hydroxide particles or complex ions concentrated near the surface of the growing coating move into breakdown channels, where they undergo transformations under the effect of high temperatures and pressure differences. Upon the extinguishing of the discharge, the formed products cover the walls and bottom of pores (breakdown channels) and form dispersed particles in them. The coating growth and increase in its thickness result in sealing such areas with the increased concentration of

Table 2. Fe/Ti atomic ratio in pores, rolls, and on the surface of coatings formed at $i = 0.05$ A/cm^2 for 5 and 10 min

Electrolyte	t, min	Phase composition	Fe/Ti		
			pores	rolls	surface
PBWFe-SO_4	5		0.5	0.5	0.6
	10	TiO_2 (a) + ?FeO(OH)	2.5	0.8	1.7
PBWFe-Citr	5		1.2	1.2	1.7
	10	TiO_2 (a)	1.6	1.9	1.7

the electrolyte components in the coating bulk, their subsequent diffusion and oxidation, and, finally, more homogeneous distribution of the electrolyte components over the coating thickness.

In view of the above, the calculated Fe/Ti atomic ratio is the same for all main formations on the surface, in spite of different contents of these metals in them (Table 2). In our opinion, the latter corroborates the suggestions that have been made regarding the mechanisms of growth of multicomponent PEO coatings.

5. CONCLUSIONS

(1) The data obtained in the present work and the available literature data demonstrate that, independently of the nature of the studied iron precursors and the alkaline electrolyte state (true solution of suspension electrolyte), in all cases, iron is predominantly concentrated in defect surface sites and PEO coatings' pores. Aside from iron, the coating pores contain other metals present in the electrolyte components or the substrate.

(2) In many cases, pores of such coatings contain dispersed particles with an increased metal content. The oxygen deficiency in coating pores and particles present in them allows assuming partial reduction state of these metals.

(3) A majority of the studied coatings exhibit ferromagnetic behavior at both low and room temperatures. The available data enable one to relate coatings' ferromagnetic properties to metals concentrated in pores, as well as in the compositions of nano- and microsized crystallites.

ACKNOWLEDGMENTS

The work was performed within the framework of a state order of the Institute of Chemistry, Far Eastern Branch, Russian Academy of Sciences, (project no. 0265-2014-0001), and was partially supported by the Russian Foundation for Basic Research (project no. 15-03-03271-a) and the Far East Branch, Russian Academy of Sciences, Program of Basic Research "Far East" (project no. 265-20-15-0022).

REFERENCES

1. Jin, F.Y., Tong, H.H., Li, J., et al., *Surf. Coat. Technol.,* 2006, vol. 201, nos. 1–2, pp. 292–295.
2. Tang, H. and Wang, F., *Mater. Sci. Technol.,* 2012, vol. 28, no. 12, pp. 1523–1526.
3. Jagminas, A., Ragalevicius, R., Mazeika, K., et al., *J. Solid State Electrochem.,* 2010, vol. 14, no. 2, pp. 271–277.
4. Rogov, A.B., Terleeva, O.P., Mironov, I.V., and Slonova, A.I., *Appl. Surf. Sci.,* 2012, vol. 258, no. 7, pp. 2761–2765.
5. Rogov, A.B., Slonova, A.I., and Mironov, I.V., *Appl. Surf. Sci.,* 2013, vol. 287, pp. 22–29.
6. Rogov, A.B., Terleeva, O.P., Mironov, I.V., and Slonova, A.I., *Prot. Met. Phys. Chem. Surf.,* 2012, vol. 48, no. 3, pp. 340–345.
7. Rudnev, V.S., Ustinov, A.Yu., Lukiyanchuk, I.V., et al., *Prot. Met. Phys. Chem. Surf.,* 2010, vol. 46, no. 5, pp. 566–572.
8. Timoshenko, A.V., Magurova, Yu.V., and Artemova, S.Yu., *Fiz. Khim. Obrab. Mater.,* 1996, no. 2, pp. 57–63.
9. Yu, X.W., Chen, L., Qin, H.L., Wu, M.Y., and Yan, Z.C., *Appl. Surf. Sci.,* 2016, vol. 366, pp. 432–438.
10. Tang, H., Xin, T.Z., Sun, Q., et al., *Appl. Surf. Sci.,* 2011, vol. 257, no. 24, pp. 10839–10844.
11. Butyagin, P.I., Khokhryakov, Ye.V., and Mamaev, A.I., *Proc. Int. Workshop "Mesomechanics: Foundations & Applications",* Tomsk, 2001, pp. 63–64.
12. Rudnev, V.S., Morozova, V.P., Lukiyanchuk, I.V., et al., *Prot. Met. Phys. Chem. Surf.,* 2013, vol. 49, no. 3, pp. 309–318.
13. Lukiyanchuk, I.V., Rudnev, V.S., Ustinov, A.Yu., et al., *Russ. J. Appl. Chem.,* 2012, vol. 85, no. 11, pp. 1686–1690.
14. Lukiyanchuk, I.V., Rudnev, V.S., Tyrina, L.M., et al., *Russ. J. Appl. Chem.,* 2009, vol. 82, no. 6, pp. 1000–1007.
15. Yao, Z.P., Hu, B., Shen, Q.X., et al., *Surf. Coat. Technol.,* 2014, vol. 253, pp. 166–170.
16. Yerokhin, A., Nie, X., Leyland, A., et al., *Surf. Coat. Technol.,* 1999, vol. 122, pp. 73–93.
17. Walsh, F.C., Low, C.T.J., Wood, R.J.K., et al., *Trans. Inst. Met. Finish.,* 2009, vol. 87, no. 3, pp. 122–135.
18. Rudnev, V.S., *Prot. Met.,* 2008, vol. 44, no. 3, pp. 263–272.
19. Kurze, P., Krysmann, W., Schreckenbach, J., et al., *Cryst. Res. Technol.,* 1987, vol. 22, no. 1, pp. 53–58.

20. Rudnev, V.S., Adigamova, M.V., Lukiyanchuk, I.V., et al., *Prot. Met. Phys. Chem. Surf.,* 2012, vol. 48, no. 5, pp. 543–552.
21. Rudnev, V.S., Lukiyanchuk, I.V., Adigamova, M.V., et al., *Surf. Coat. Technol.,* 2015, vol. 269, pp. 23–29.
22. Adigamova, M.V., Rudnev, V.S., Lukiyanchuk, I.V., et al., *Prot. Met. Phys. Chem. Surf.,* 2016, vol. 52, no. 3, pp. 526–531.
23. Rudnev, V.S., Morozova, V.P., Lukiyanchuk, I.V., et al., *Russ. J. Phys. Chem. A,* 2014, vol. 88, no. 5, pp. 863–869.
24. Rudnev, V.S., Gordienko, P.S., Kurnosova, A.G., and Orlova, T.I., RF Patent 1783004, *Byull. Izobret.,* 1992, no. 47.
25. Grilikhes, S.Ya., *Obezzhirivanie, travlenie i polirovanie metallov* (Degreasing, Etching and Polishing of Metals), Leningrad: Mashinostroenie, 1977.
26. *Chimica: Ein Wissensspeicher,* Leipzig: VEB Deutscher Verlag für Grundstoffindustrie, 1972.
27. Pechenyuk, S.I. and Kalinkina, E.V., *Zh. Fiz. Khim.,* 1993, vol. 67, no. 6, pp. 1251–1254.
28. Vassileva, E., Proinova, I., and Hadjiivanov, K., *Analyst,* 1996, vol. 121, no. 5, pp. 607–612.
29. Stremilova, N.N., Viktorovskii, I.V., and Zigel', V.V., *Russ. J. Gen. Chem.,* 2001, vol. 71, no. 1, pp. 19–22.
30. Hunterszultze, A. and Betts, G., *Elektroliticheskie kondensatory* (Electrolytic Capacitors), Moscow: Oborongiz, 1938.
31. Tareev, B.M. and Lerner, M.M., *Oksidnaya izolyatsiya* (Oxide Insulation), Moscow–Leningrad: Energiya, 1964.
32. Rudnev, V.S., *Prot. Met.,* 2007, vol. 43, no. 3, pp. 275–280.
33. Snezhko, L.A. and Chernenko, V.I., *Elektron. Obrab. Mater.,* 1983, no. 4, pp. 38–40.
34. Vovna, V.I., Gnedenkov, S.V., Gordienko, P.S., et al., *Russ. J. Electrochem.,* 1998, vol. 34, no. 10, pp. 1090–1093.
35. Rudnev, V.S., Vaganov-Vil'kins, A.A., Ustinov, A.Yu., and Nedozorov, P.M., *Prot. Met. Phys. Chem. Surf.,* 2011, vol. 47, no. 3, pp. 330–338.
36. Rudnev, V.S., Tyrina, L.M., Ustinov, A.Yu., et al., *Kinet. Catal.,* 2010, vol. 51, no. 2, pp. 266–272.
37. Curran, J. and Clyne, T., *Acta Mater.,* 2006, vol. 54, pp. 1985–1993.
38. Snizhko, L.O., *Prot. Met. Phys. Chem. Surf.,* 2014, vol. 50, no. 6, pp. 705–708.
39. Li, Y., Shimada, H., Sakairi M., et al., *J. Electrochem. Soc.,* 1997, vol. 144, no. 3, pp. 866–876.
40. Cheng, Y.L., Gao J.H., Mao, M., et al., *Surf. Coat. Technol.,* 2016, vol. 291, pp. 239–249.

Translated by D. Marinin